



HAL
open science

Kinetic modeling using temperature as an on-line measurement: Application to the hydrolysis of acetic anhydride, a revisited kinetic model

Elizabeth Antonia Garcia-Hernandez, Camilla Ribeiro Souza, Lamiae Vernières-Hassimi, Sébastien Leveneur

► To cite this version:

Elizabeth Antonia Garcia-Hernandez, Camilla Ribeiro Souza, Lamiae Vernières-Hassimi, Sébastien Leveneur. Kinetic modeling using temperature as an on-line measurement: Application to the hydrolysis of acetic anhydride, a revisited kinetic model. *Thermochimica Acta*, 2019, 682, pp.178409. 10.1016/j.tca.2019.178409 . hal-02435541

HAL Id: hal-02435541

<https://normandie-univ.hal.science/hal-02435541>

Submitted on 21 Dec 2021

HAL is a multi-disciplinary open access archive for the deposit and dissemination of scientific research documents, whether they are published or not. The documents may come from teaching and research institutions in France or abroad, or from public or private research centers.

L'archive ouverte pluridisciplinaire **HAL**, est destinée au dépôt et à la diffusion de documents scientifiques de niveau recherche, publiés ou non, émanant des établissements d'enseignement et de recherche français ou étrangers, des laboratoires publics ou privés.



Distributed under a Creative Commons Attribution - NonCommercial 4.0 International License

1 **Kinetic modeling using temperature as an on-line measurement:**
2 **Application to the hydrolysis of acetic anhydride, a revisited kinetic model.**

3 *Elizabeth Antonia Garcia-Hernandez¹, Camilla Ribeiro Souza¹, Lamiae Vernières-Hassimi¹,*
4 *Sébastien Leveneur^{*1,2}*

5 ¹*Normandie Univ, INSA Rouen, UNIROUEN, LSPC, EA4704, 76000 Rouen, France, E-mail:*
6 *sebastien.leveneur@insa-rouen.fr*

7 ²*Laboratory of Industrial Chemistry and Reaction Engineering, Johan Gadolin Process*
8 *Chemistry Centre, Åbo Akademi University, Biskopsgatan 8, FI-20500 Åbo/Turku, Finland.*

9 **Abstract.** The use of calorimeter in chemical reaction engineering is a powerful tool to
10 estimate kinetic constants. Indeed, reaction temperature is used as an online analytical signal.
11 Nevertheless, the thermal characterization of the calorimeter must be done to avoid wrong
12 estimation. The hydrolysis of acetic anhydride was used as a reaction model in a handmade
13 calorimeter, because it is a fast and exothermic reaction. Several research groups have studied
14 this reaction without taking into account the autocatalytic effect due to the production of acetic
15 acid. To fill this gap, a kinetic model was developed by taking this phenomenon and in a
16 thermally characterized handmade calorimeter. The estimated kinetic constants in the
17 handmade calorimeter were found to be similar than in the established calorimeter Mettler
18 Toledo RC1.

19 **KEYWORDS:** calorimeter, exothermic reaction, isoperibolic mode, kinetic modeling.

20

21 **HIGHLIGHTS**

22 Thermal characterization of a calorimeter

23 Kinetic model using reaction temperature as online observable

24 Kinetic model for acetic anhydride hydrolysis taking into account autocatalytic effect

25

26

27 1.INTRODUCTION

28 Calorimetry is a science that finds its roots with the works of Joseph Black, Antoine Lavoisier
29 and Pierre-Simon Laplace. It is an important thermal analytical tool in different fields such as
30 material science, polymer, chemistry or chemical engineering. One can get fundamental
31 thermal and thermodynamic data of different compounds by using different thermal modes.

32 In chemical engineering, calorimetry allows to measure/estimate specific heat capacities of
33 chemicals [1–4] and reaction enthalpies [5–7] . It is also the appropriate tool in process safety
34 and more particularly in thermal risk assessment to determine risk parameters such as time-to-
35 maximum-rate under adiabatic conditions TMR_{ad} or adiabatic temperature rise ΔT_{ad} . The
36 knowledge of these safety parameters allow to evaluate the thermal risk of a chemical process
37 [7–12] .

38 Another benefit of calorimeter is in chemical reaction engineering, where reaction temperature
39 is used as an online measurement signal. The use of calorimeter to estimate rate constants has
40 significantly increased these last years, essentially for fast and exothermic reactions.

41 The use of reaction temperature or heat-flow rate released as online signals to evaluate the
42 kinetics of a reaction was used by several research groups [13–19] . The development of
43 calorimeters has participated to the development of this approach. Nevertheless, one should
44 also take into account different thermal phenomena such as specific heat capacity of the inserts
45 or heat loss [16] .

46 Hydrolysis of acetic anhydride is frequently used as a calibration reaction for calorimeters
47 [13,20]. This reaction was studied by several research groups:

48 -Wiseman [21] used pH as an online analytical method but he did not include the energy
49 balance,

50 -Susanne et al. [22] used NMR as an online method but they did not include energy balance,

51 -Hirota et al.[23] have used the temperature to make the kinetic estimation without taking into
52 account the autocatalytic effect of the reaction,

53 -Zogg et al. [24,25] studied this reaction by combining calorimetric and IR techniques, but they
54 assumed a first order reaction,

55 -Gomez Garcia et al. [26] used this reaction as an example for thermal stability,

56 -Asiedu et al. [27] studied this reaction under adiabatic mode but with a first order approach.

57 This reaction is known to be autocatalytic due to the dissociation of the product acetic acid.
58 Nevertheless, none of these research groups have developed a kinetic model taking into
59 account this phenomenon for this reaction.

60 The objective of this article is to develop a kinetic model including the autocatalytic effect and
61 the different thermal phenomena. To estimate the kinetic constants, experiments under
62 isoperibolic mode was performed in a hand-made calorimeter. The thermal properties of this
63 calorimeter were investigated. To validate the developed kinetic model in the hand-made
64 calorimeter, a comparison with the RC1 Mettler-Toledo calorimeter was done.

65

66

67 **2.EXPERIMENTAL SECTION**

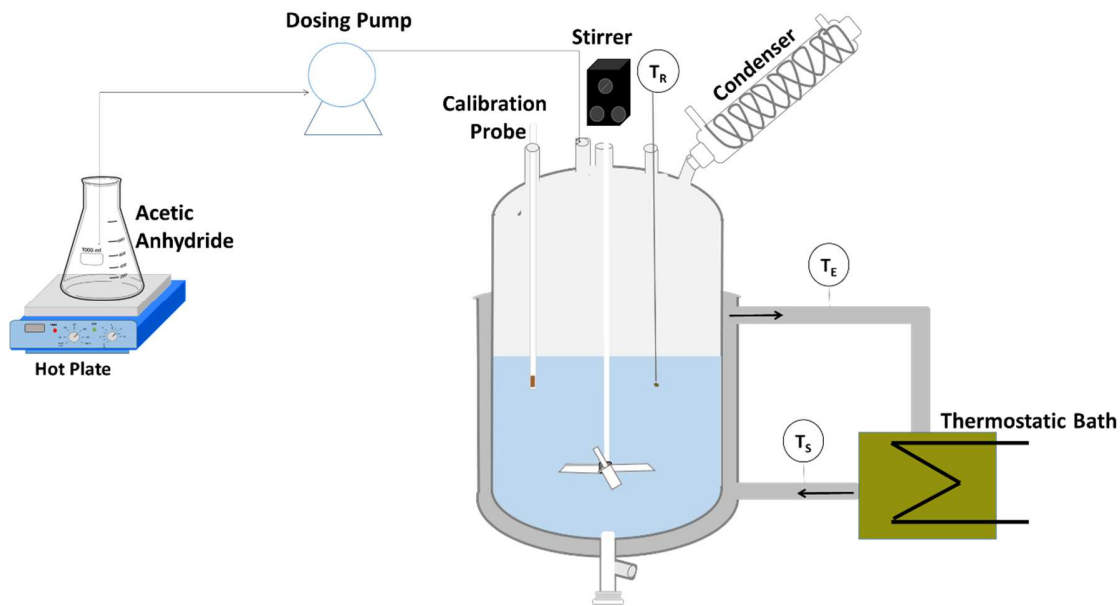
68 2.1. Materials

69 The following chemicals were used: ACS reagent acetic anhydride (purity $\geq 99\%$) and
70 distilled water.

71 2.2. Experimental Setup

72 Kinetic experiments for the hydrolysis of acetic anhydride were carried out in the hand-made
73 calorimeter composed of a 300 mL jacketed glass reactor equipped with accurate temperature
74 probes, a calibration probe to measure the global heat transfer coefficient, a mechanical stirrer
75 and reflux condenser. The internal diameter of the jacketed reactor was 10 cm, and the
76 mechanical stirrer was a pitched blade turbine impeller (diameter 3.8 cm and 4 blades). The
77 inlet temperature of condenser was fixed at 10°C to avoid the loss of liquid phase compounds.
78 Experiments were performed under isoperibolic and semi-batch mode. Fig. 1 shows a
79 simplified scheme of the reactor setup.

80



81

82

Fig. 1. Schematic representation of the experimental setup.

83

84 2.3 Thermal characterization of the calorimeter

85 The goals of these experiments are to measure the heat transfer coefficient between the
 86 reaction mixture and heat carrier, evaluate the heat loss and measure the specific heat
 87 capacities of the inserts.

88 - Measurement of heat transfer coefficient

89 To determine the heat transfer coefficient, an electrical calibration was used. For that, the
 90 reactor was filled with a solution and heated to the desired temperature in the absence of
 91 reaction and under isoperibolic conditions. When the solution temperature was stable, a known
 92 electrical power (Joule heating) was provided for around 10 minutes and then switched off.
 93 The evolution of the solution temperature was recorded. One can find a detailed description of
 94 this method in previous article of our group [28,29].

95 - Measurement of specific heat capacity of the inserts.

96 The procedure described in reference [30] was used. The thermostatic bath was set to a
97 temperature but the heat carrier did not circulate in the reactor jacket. At the same time the
98 reactor was filled with water at room temperature. When the thermostatic bath reached the
99 desired temperature, the pump system was switched on to allow the circulation of the heat
100 carrier in the jacket. Both temperature, jacket and water temperature were recorded. These
101 measurements were carrying out at three different temperatures (40, 60 and 80 °C).

102 - Evaluation of heat loss

103 The thermostatic bath was set at a temperature and the circulation of the heat carrier was
104 switched on. The reactor was filled with water and heated to the desired temperature. When the
105 water temperature was at the same temperature as the jacket one, the circulation of the heat
106 carrier stopped (defined as time zero) and removed from the jacket. The water temperature was
107 recorded. The experiments were carrying out at three different temperatures (40, 60 and 80 °C).

108 2.4 Kinetic experiments in calorimeter

109 Kinetic experiments were performed in semi-batch mode where acetic anhydride was added
110 into the reactor. Table 1 shows the experimental matrix.

111

112

113

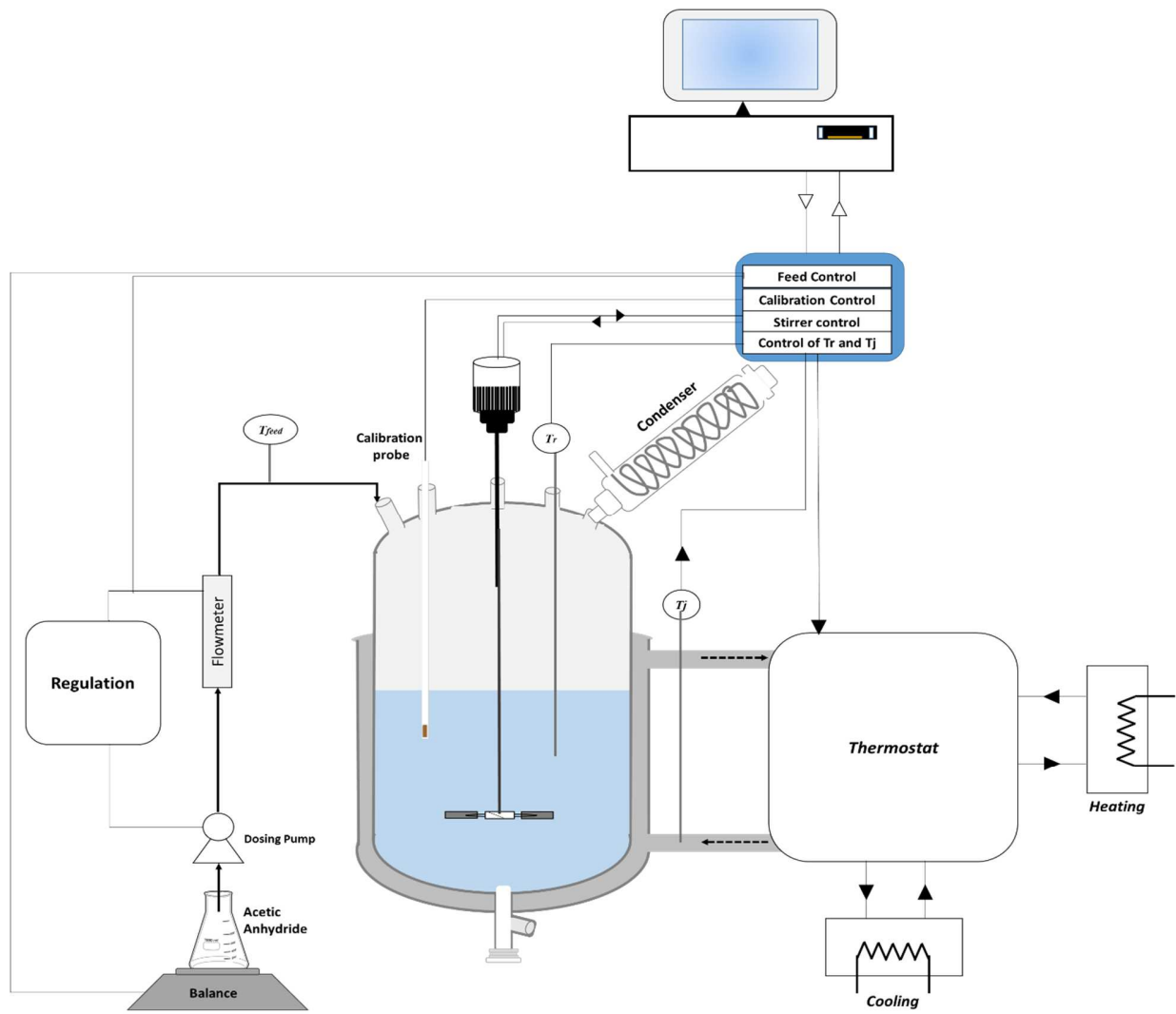
114 **Table 1**
115 Experimental matrix in handmade calorimeter with an agitation speed of 400 rpm.

RUN	Added volume of acetic anhydride (L)	Time of addition (s)	Acetic anhydride volumetric flow rate (L s⁻¹)	Initial volume of water (L)	Initial jacket and reaction temperature (°C)	Feed temperature (°C)
1	0.09	7.00	0.0128	0.19	30.07	27.00
2	0.09	7.00	0.0128	0.19	39.73	28.00
3	0.09	7.00	0.0128	0.19	49.34	48.00
4	0.09	7.00	0.0128	0.19	59.17	58.00
5	0.13	600.00	0.0002	0.14	49.58	23.00

116

117 2.5 Kinetic experiment in Mettler Toledo calorimeter RC1

118 The Mettler™ RC1 is a jacketed-glass reactor calorimeter of 2 L presented in Fig. 2. It is
119 equipped with a Pt100 temperature probe, an electrical calibration heating and a feed system (a
120 dosing pump and a balance, with measurement of the feed temperature). The heating-cooling
121 system works within a temperature range of -15 to +200°C. WinRCNT software solves the
122 energetic balance on the reaction mass.



123

124

125

126

127

128

Fig. 2. Schematic representation of the reaction calorimeter RC1.

129 **Table 2**

130 Experimental matrix for acetic anhydride hydrolysis in RC1 calorimeter with an agitation

131 speed of 400 rpm.

132

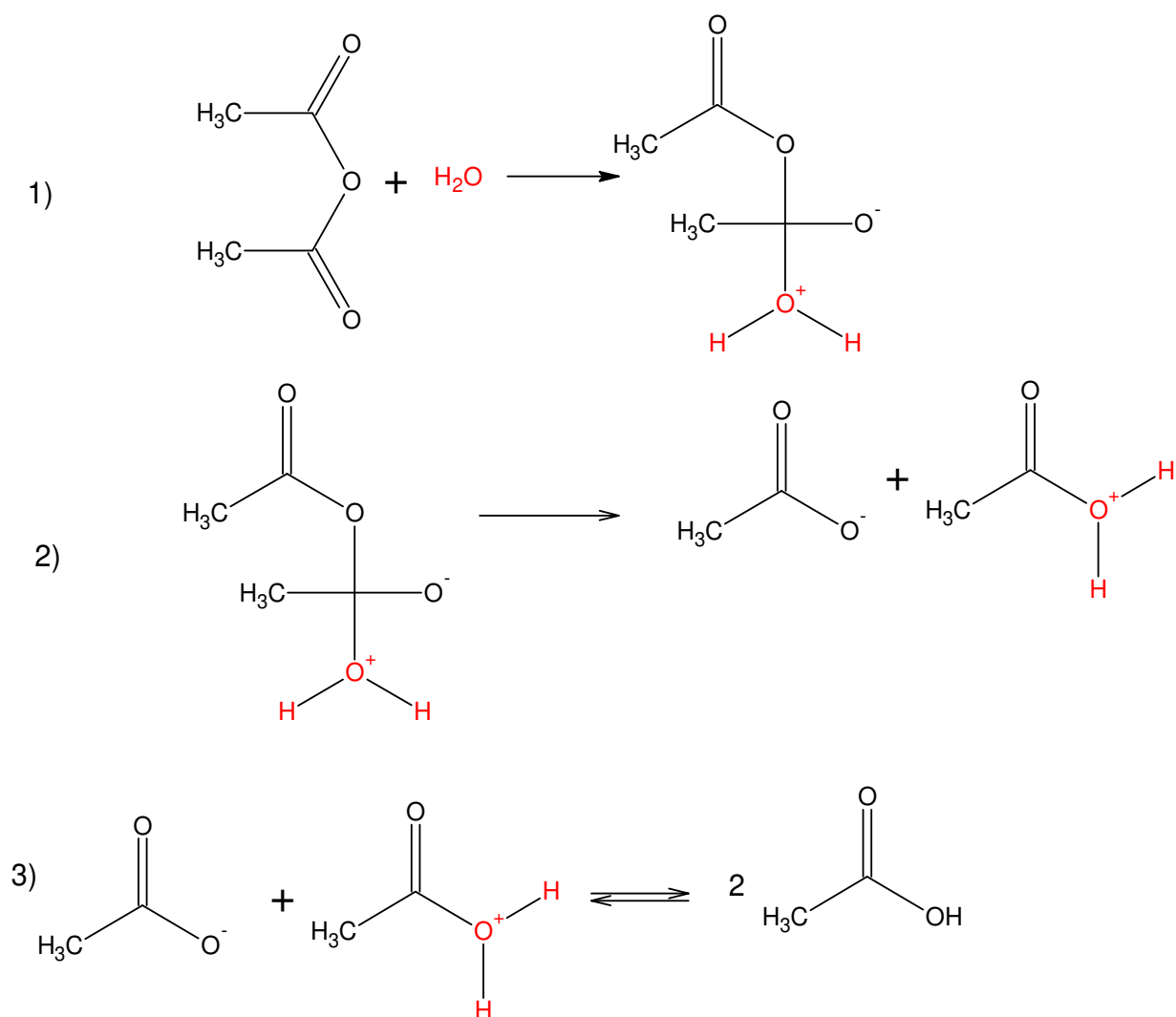
RUN	Added volume of acetic anhydride (L)	Time of addition (s)	Acetic anhydride volumetric flow rate (Ls⁻¹)	Initial volume of water (L)	Initial jacket and reaction temperature (°C)	Feed temperature (°C)
6	0.2295	300	0.0007	1.2000	39.88	22.86
7	0.464	300	0.0015	0.9658	39.87	22.20

133

134 **3. RESULTS AND DISCUSSION**

135 3.1 Kinetics

136 To take into account the autocatalysis effect of acetic anhydride hydrolysis, the reaction can be
 137 divided in two routes: catalyzed and non-catalyzed one. Fig. 3 shows the non-catalyzed
 138 reaction mechanism.



139
140

Fig. 3. Non-catalyzed reaction mechanism.

141

142 From Fig. 3, the rate-determining step can be assumed to be step 1. Thus, the non-catalyzed
143 hydrolysis rate can be expressed as:

$$144 R_{Hydrolysis-non.cat} = k_{Hydrolysis-non.cat} \times [Anhydride\ Acetic] \times [H_2O] \quad (1)$$

145 Fig. 4 shows the reaction mechanism by the catalyzed route.

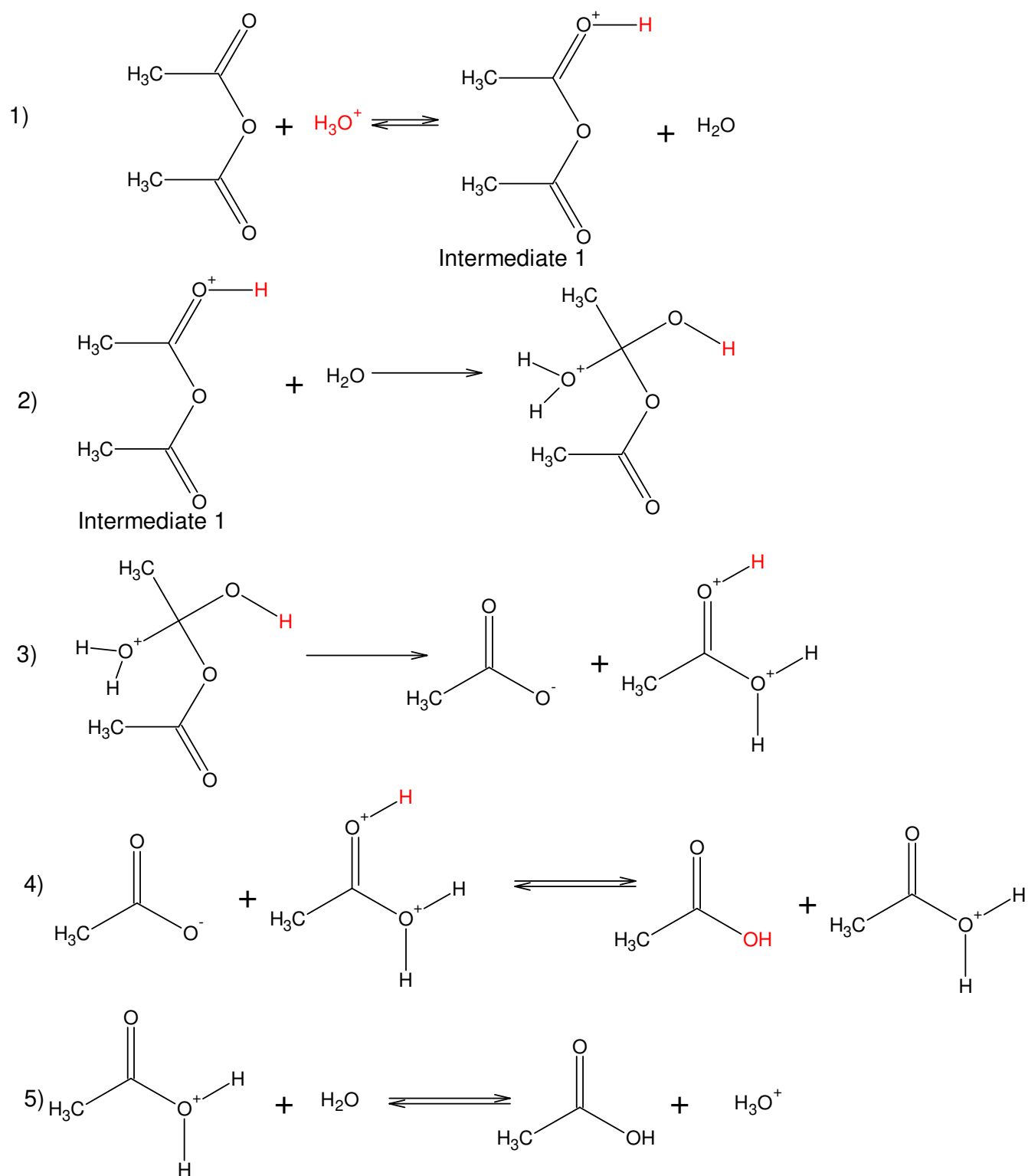


Fig. 4. Catalyzed reaction mechanism.

148 Reaction 2 (Fig. 4) is assumed to be the rate determining step, thus the rate of catalyzed
 149 hydrolysis can be expressed as

$$150 \quad R_{Hydrolysis-cat} = k_{Hydrolysis-cat} \times [Intermediate_1] \times [H_2O] \quad (2)$$

151 Steady-state approximation is applied on reaction 1 (Fig. 4), thus one gets

$$152 \quad K_1 = \frac{[Intermediate_1] \times [H_2O]}{[Acetic\ anhydride] \times [H_3O^+]} \quad (3)$$

153 By combining Eqs (2) and (3), one gets:

$$154 \quad R_{Hydrolysis-cat} = k_{Hydrolysis-cat} \times K_1 \times \frac{[Acetic\ anhydride] \times [H_3O^+]}{[H_2O]} \times [H_2O] \quad (4)$$

155 Hence, by adding Eqs (1) and (4), the rate of hydrolysis becomes

$$156 \quad R_{Hydrolysis} = R_{Hydrolysis-non.cat} + R_{Hydrolysis-cat}$$

$$157 \quad = ([Acetic\ anhydride] \times [H_2O]) \times \left[k_{Hydrolysis-non.cat} + k_{Hydrolysis-cat} \times K_1 \times \frac{[H_3O^+]}{[H_2O]} \right] \quad (5)$$

158 By noting $k'_{Hydrolysis-cat} = k_{Hydrolysis-cat} \times K_1$, then eq (5) becomes

$$159 \quad R_{Hydrolysis} = ([Acetic\ anhydride] \times [H_2O]) \times \left[k_{Hydrolysis-non.cat} + k'_{Hydrolysis-cat} \frac{[H_3O^+]}{[H_2O]} \right]$$

160 (6)

161 Both rate constants were estimated in this study.

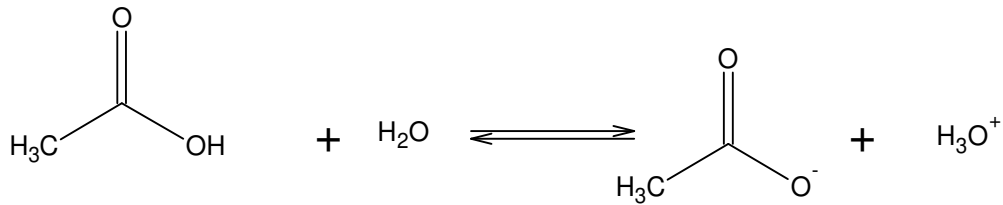
162

163

164

165 3.2 Sources of hydroxonium ion

166 The autoprotolysis of water was neglected in this study. The source of hydroxonium ion was
 167 mainly due to the dissociation of the product acetic acid as illustrated by Scheme 1.



168

169 Scheme 1. Dissociation of acetic acid.

170

171 Mass balance of the organic species gives

$$172 \quad [\textit{Acetic anhydride}]_{FEED} = [\textit{Acetic anhydride}] + \frac{1}{2} \cdot [\textit{Acetic acid}] + \frac{1}{2} \cdot [\textit{CH}_3\textit{COO}^-] \quad (7)$$

173 The dissociation of acetic acid is fast, thus the dissociation constant, $K_{Acetic\ acid}^C$, can be
 174 expressed as

$$175 \quad K_{Acetic\ acid}^C = \frac{[\textit{CH}_3\textit{COO}^-] \times [\textit{H}_3\textit{O}^+]}{[\textit{CH}_3\textit{COOH}] \times [\textit{H}_2\textit{O}]} = \frac{K_{Acetic\ acid}^T}{55.56} \quad (8)$$

176 $K_{Acetic\ acid}^T$ is the true thermodynamic constant expressed according to Sue et al. [31].

177 According to the electroneutrality principle, the concentration of cation and anion species are
 178 the same.

$$179 \quad [\textit{H}_3\textit{O}^+] \approx [\textit{CH}_3\textit{COO}^-] \quad (9)$$

180 By combining Eqs (8) and (9), the acetic acid concentration can be expressed as

$$181 \quad [\textit{CH}_3\textit{COOH}] = \frac{[\textit{H}_3\textit{O}^+]^2}{K_{Acetic\ acid}^C \times [\textit{H}_2\textit{O}]} \quad (10)$$

182 Eqs (10) and (9) are introduced in Eq (7) leading to

$$183 \quad [Acetic\ anhydride]_{FEED} = [Acetic\ anhydride] + \frac{1}{2} \cdot \frac{[H_3O^+]^2}{K_{Acetic\ acid}^C \times [H_2O]} + \frac{1}{2} \cdot [H_3O^+]$$

184 equivalent to

$$185 \quad \frac{1}{2} \cdot \frac{[H_3O^+]^2}{K_{Acetic\ acid}^C \times [H_2O]} + \frac{1}{2} \cdot [H_3O^+] + [Acetic\ anhydride] - [Acetic\ anhydride]_{FEED} = 0$$

$$186 \quad (11)$$

187 By taking into account only the positive roots of Eq (11), one gets

$$188 \quad [H_3O^+] = K_{Acetic\ acid}^C \cdot [H_2O] \cdot \left[-\frac{1}{2} + \sqrt{\frac{1}{4} - \frac{2}{K_{Acetic\ acid}^C \times [H_2O]} \cdot ([Acetic\ anhydride] - [Acetic\ anhydride]_{FEED})} \right]$$

$$189 \quad (12)$$

190

191

192

193

194

195

196

197 3.3 Mass balances

198 As mentioned in the experimental section, experiments were performed in semi-batch mode
199 with the addition of acetic anhydride in the reactor.

200 Mass balances for acetic anhydride, acetic acid and water lead to the following ordinary
201 differential equations:

202
$$\frac{d[Acetic\ anhydride]}{dt} = \frac{Q}{V_R} \times ([Acetic\ anhydride]_{FEED} - [Acetic\ anhydride]) - R_{Hydrolysis}$$

203 (13)

204
$$\frac{d[Water]}{dt} = -[Water] \times \frac{Q}{V_R} - R_{Hydrolysis} \quad (14)$$

205
$$\frac{d[Acetic\ acid]}{dt} = -[Acetic\ acid] \times \frac{Q}{V_R} + 2 \times R_{Hydrolysis} \quad (15)$$

206
$$\frac{dV_R}{dt} = Q \quad (16)$$

207 where, Q is the volumetric flow rate, $[Acetic\ anhydride]_{FEED}$ is the concentration of acetic
208 anhydride in the feed.

209

210

211

212 3.4 Energy balance

213 For a semi-batch reactor under isoperibolic conditions, energy balance on the reaction mixture
 214 phase can be expressed as [28,32]:

$$\begin{aligned}
 215 \quad q_{acc} &= q_{reaction} + q_{exchange\ with\ heat\ carrier} + q_{loss} + q_{dosing} + q_{solvation} \\
 216 \quad \Leftrightarrow (m_R \cdot \widehat{C}_{P_R} + m_{ins} \cdot \widehat{C}_{P_{ins}}) \times \frac{dT_R}{dt} &= -R_{Hydrolysis} \times V_R \times \Delta H_{R,Hydrolysis} + U \times A \times \\
 217 \quad (T_j - T_R) + UA_{loss} \times (T_{ambient} - T_R) + Q \times \overline{C_{P_{Acetic\ Anhydride}}} \times [Acetic\ anhydride]_{FEED} \times \\
 218 \quad (T_{FEED} - T_R) - \frac{\Delta H_{solvation} \times Q}{V_{molar} \times (Acetic\ Anhydride)} \\
 219 \quad (17)
 \end{aligned}$$

220 Heat capacities of the different species at stake were estimated by using Aspen Plus and the
 221 UNIQUAC thermodynamic model. Each term of Eq (17) is explained below.

222 *Accumulated heat-flow rate $q_{acc} = (m_R \cdot \widehat{C}_{P_R} + m_{ins} \cdot \widehat{C}_{P_{ins}}) \times \frac{dT_R}{dt}$

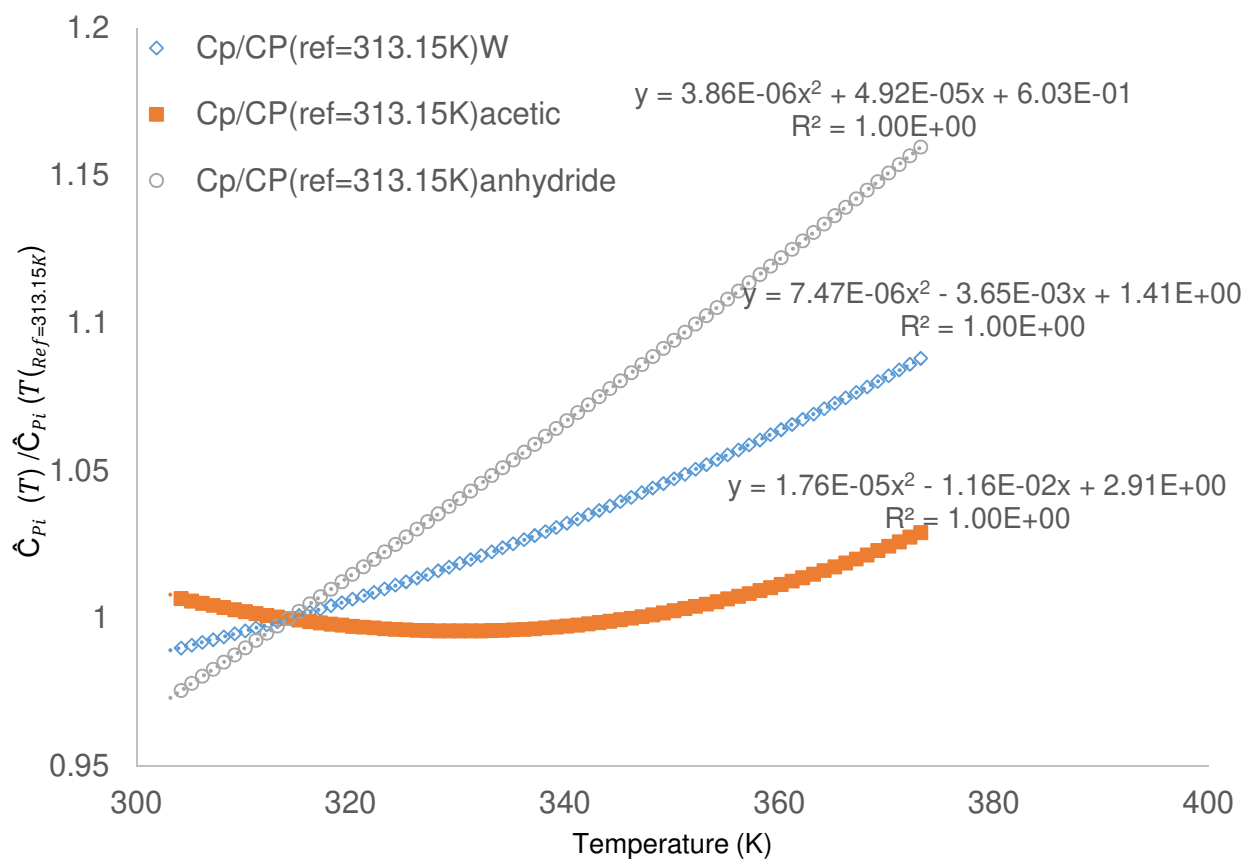
223 The specific heat capacity of the reaction mixture \widehat{C}_{P_R} (J.kg⁻¹.K⁻¹) can be expressed as

$$\begin{aligned}
 224 \quad \widehat{C}_{P_R} &= \omega_W \times \widehat{C}_{P_W} + \omega_{Acetic\ anhydride} \times \widehat{C}_{P_{Acetic\ anhydride}} + \omega_{Acetic\ acid} \times \widehat{C}_{P_{Acetic\ acid}} \\
 225 \quad (18)
 \end{aligned}$$

226 The specific heat capacity of a compound with temperature can be expressed as

$$227 \quad \frac{\widehat{C}_{P_i}(T)}{\widehat{C}_{P_i}(T_{Ref})} = A.T^2 + B.T + C \quad (19)$$

228 Fig. 5 shows the evolution of $\frac{\widehat{C}_{P_i}(T)}{\widehat{C}_{P_i}(T_{Ref=313.15K})}$ for water, acetic anhydride and acetic acid based
 229 on AspenPlus database.



230

231

Fig. 5. $\frac{\hat{C}_{P_i}(T)}{\hat{C}_{P_i}(T_{Ref=313.15K})}$ versus temperature T/K.

232

233

234 **Table 3**

235 Specific heat capacity parameters.

236

	Water	Acetic acid	Acetic anhydride
Cp(313.15K)	4.18008	1.33385	1.63724
A	7.47E-06	1.76·10 ⁻⁰⁵	3.86·10 ⁻⁰⁶
B	-0.0036	-0.0116	5.00·10 ⁻⁰⁵
C	1.4081	2.911	0.6032

237 The evaluation of the term $m_{ins} \cdot \widehat{C}_{P_{ins}}$ is detailed in chapter 3.5. Reactor characteristic.

238 *Heat-flow rate due to chemical reaction $q_{reaction} = -R_{Hydrolysis} \times V_R \times \Delta H_{R,Hydrolysis}$

239 From Zogg et al. [24], the enthalpy of hydrolysis, $\Delta H_{R,Hydrolysis}$, can be estimated to be equal
240 to -60 kJ/mol. The term V_R stands for the reaction volume.

241 *Heat-flow rate exchange with heat carrier $q_{exchange\ with\ heat\ carrier} = U \times A \times (T_j - T_R)$

242 In chapter 3.5, the determination of U and A is explained. The terms T_j and T_R are the jacket
243 and reaction temperatures, respectively.

244 *Heat flow rate loss $q_{loss} = UA_{loss} \times (T_{ambient} - T_R)$

245 The estimation of this loss is explained in chapter 3.5.

246 *Heat flow rate due to dosing $q_{dosing} = Q \times \overline{C_{P_{Acetic\ Anhydride}}} \times [Acetic\ anhydride]_{FEED} \times (T_{FEED} - T_R)$

247 where, $\overline{C_{P_{Acetic\ Anhydride}}}$ ($J\ mol^{-1}\ K^{-1}$) is the molar heat capacity of acetic anhydride. The

248 concentration of acetic anhydride in the feed is $[Acetic\ anhydride]_{FEED} = 10.58\ mol.\ L^{-1}$.

249 The term Q is the feeding volumetric flow-rate.

250 *Heat flow rate of solvation $q_{solvation} = -\frac{\Delta H_{solvation} \times Q}{V_{molar} \times (Acetic\ Anhydride)}$

251 From Zogg et al. [24], the heat of solvation of acetic anhydride $\Delta H_{solvation}$ is equal to + 3000

252 J/mol when the reaction temperature is higher than 40°C. The molar volume of acetic

253 anhydride is equal to 0.0944 L mol⁻¹ [33].

254

255 3.5 Reactor characteristic

256 The relationship between the reaction volume and the surface A was found to be

257
$$A(m^2) = 0.0817 \times V(L) \quad (21)$$

258 To evaluate the heat transfer coefficient U during the reaction, one can use the sum of thermal
259 resistances using the thin wall approximation [34-35] .

260
$$\frac{1}{U} = \frac{1}{h_R} + \frac{d_{Wall}}{\lambda_{Wall}} + \frac{1}{h_j} \quad (22)$$

261 where, $\frac{1}{h_R}$ and $\frac{1}{h_j}$ represent the convective resistance to the heat transfer from the reaction side

262 and jacket side, respectively; d_w is the thickness of the glass wall between reaction mixture and

263 the heat carrier fluid, and λ_{Wall} is the heat conductivity of the glass wall.

264 The term $\frac{1}{h_R}$ can change during the reaction, and the term $\frac{d_{Wall}}{\lambda_{Wall}} + \frac{1}{h_j}$ can be merged to a

265 constant and noted by $\frac{1}{\varphi_R}$. Eq. (22) becomes now:

266
$$\frac{1}{U} = \frac{1}{h_R} + \frac{1}{\varphi_R} \quad (23)$$

267 Under isothermal conditions and in the absence of chemical reactions, the properties of the

268 fluid and geometrical factors are constant. Thus the internal heat transfer coefficient can be

269 expressed as

270
$$\frac{1}{h_R} = Const \times \left(\frac{\mu_R}{\rho_R^2 \times \hat{C}_{P_R} \times \lambda_R^2} \right)^{1/3} \times \left(\frac{d_R^3}{d_c^2} \right)^{1/3} \times \left(\frac{1}{N^2} \right)^{1/3} \quad (24)$$

271 where,

272 Const is a constant,

273 μ_R is the dynamic viscosity of the reaction mixture in $\text{kg m}^{-1} \text{s}^{-1}$,

274 ρ_R is the density of the reaction mixture in kg m^{-3} ,

275 \hat{C}_{pR} is the specific heat capacity of the reaction mixture in $\text{J kg}^{-1} \text{K}^{-1}$,

276 λ_R is the thermal conductivity of the reaction mixture in $\text{W m}^{-1} \text{K}^{-1}$,

277 d_R is the reactor diameter in m,

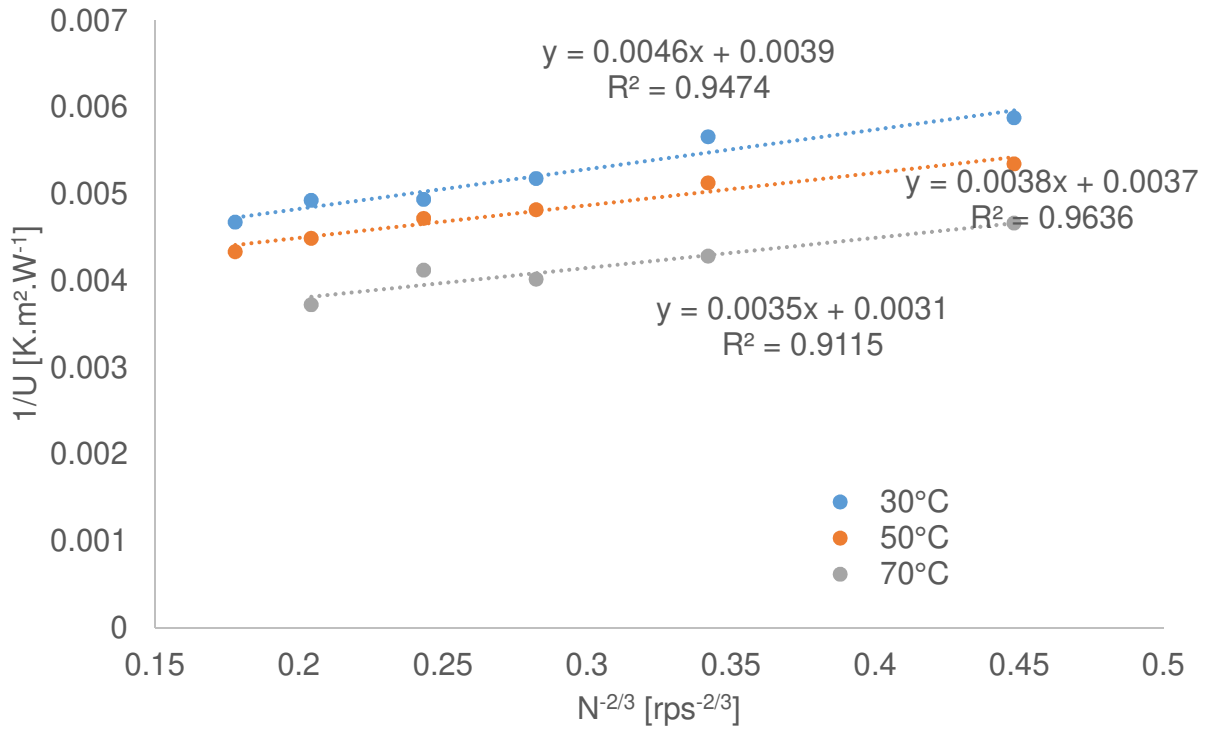
278 N is the rotating speed in round per second,

279 d_s is the stirrer diameter in m.

280 Fig. 6 shows the evolution of $\frac{1}{U}$ versus $\left(\frac{1}{N^2}\right)^{1/3}$, also known as Wilson plot. To evaluate the

281 values of $\frac{1}{\varphi_R}$ and $\frac{1}{h_R}$, a mixture containing 56 wt% of acetic acid was used as a representative

282 one.



283

284 Fig. 6. Wilson plot $1/U$ versus $N^{-2/3}$ with a weight percentage of acetic acid of 56 %.

285

286 From Fig. 6, the values of $\frac{1}{\varphi_R}$ and $\frac{1}{h_R}$ can be assumed temperature independent. The values of

287 $\frac{1}{\varphi_R}$ is evaluated to 0.0035 K m² W⁻¹ and $\frac{1}{h_R}$ to 0.0011 K m² W⁻¹ at 400 rpm.

288

289 *Determination of specific heat capacity of inserts

290 In the absence of chemical reactions, the energy balance can be expressed as

291
$$\left(m_R \cdot \widehat{C}_{P_R} + m_{ins} \cdot \widehat{C}_{P_{ins}}\right) \times \frac{dT_R}{dt} = U \times A \times (T_j - T_R) \quad (26)$$

292 By assuming that specific heat capacity is constant on small temperature range, thus Eq. (26)

293 can be integrated as

294
$$\ln \frac{T_R - T_j}{T_{R0} - T_{j0}} = \frac{-U \times A}{(m_R \cdot \widehat{C}_{P_R} + m_{ins} \cdot \widehat{C}_{P_{ins}})} \times t \quad (27)$$

295 The term $m_{ins} \cdot \widehat{C}_{P_{ins}}$ was equal to 29.95 J K⁻¹.

296 *Determination of the heat loss q_{loss}

297 Heat losses may then occur on the top side and on lateral or jacket side. Assuming a same heat

298 loss coefficient on both sides, since heat losses are limited by external natural convection on

299 both areas, the energy balance can then be described by

300
$$\left(m_R \cdot \widehat{C}_{P_R} + m_{ins} \cdot \widehat{C}_{P_{ins}}\right) \times \frac{dT_R}{dt} = UA_{loss} \times (T_{ambient} - T_R) \quad (28)$$

301 By assuming that heat capacity and UA_{loss} is temperature independent, thus Eq. (28) becomes

302
$$\ln \frac{T_R - T_{ambient}}{T_{R0} - T_{ambient0}} = \frac{-UA_{loss}}{(m_R \cdot \widehat{C}_{P_R} + m_{ins} \cdot \widehat{C}_{P_{ins}})} \times t \quad (29)$$

303 We have found that UA_{loss} is equal to 0.053 W K⁻¹.

304

305 3.6 Modeling stage.

306 The system of ordinary differential Eqs (13)-(17) were solved out by the ODESSA solver.

307 Reaction temperature was used as an observable.

308 Simplex and Levenberg-Marquardt algorithms were used to estimate the kinetic constants

309 ($k'_{Hydrolysis-cat}(T_{ref})$; $Ea_{Hydrolysis-cat}$; $k_{Hydrolysis-non.cat}(T_{ref})$ and $Ea_{Hydrolysis-non.cat}$ ·

310 The rate constants at a temperature T were estimated by using a modified Arrhenius equation:

311
$$k'_{Hydrolysis-cat}(T) = k'_{Hydrolysis-cat}(T_{ref}) \times \exp\left(\frac{-Ea_{Hydrolysis-cat}}{R} \times \left(\frac{1}{T} - \frac{1}{T_{ref}}\right)\right) \quad (30)$$

312
$$k_{Hydrolysis-non.cat}(T) = k_{Hydrolysis-non.cat}(T_{ref}) \times \exp\left(\frac{-Ea_{Hydrolysis-non.cat}}{R} \times \left(\frac{1}{T} - \frac{1}{T_{ref}}\right)\right)$$

313 (31)

314 The solver and algorithms were implemented in the software ModEst [36]. The optimization

315 algorithms minimized the following objective function ω

316
$$\omega = (y_{exp} - y_{model})^2 \quad (32)$$

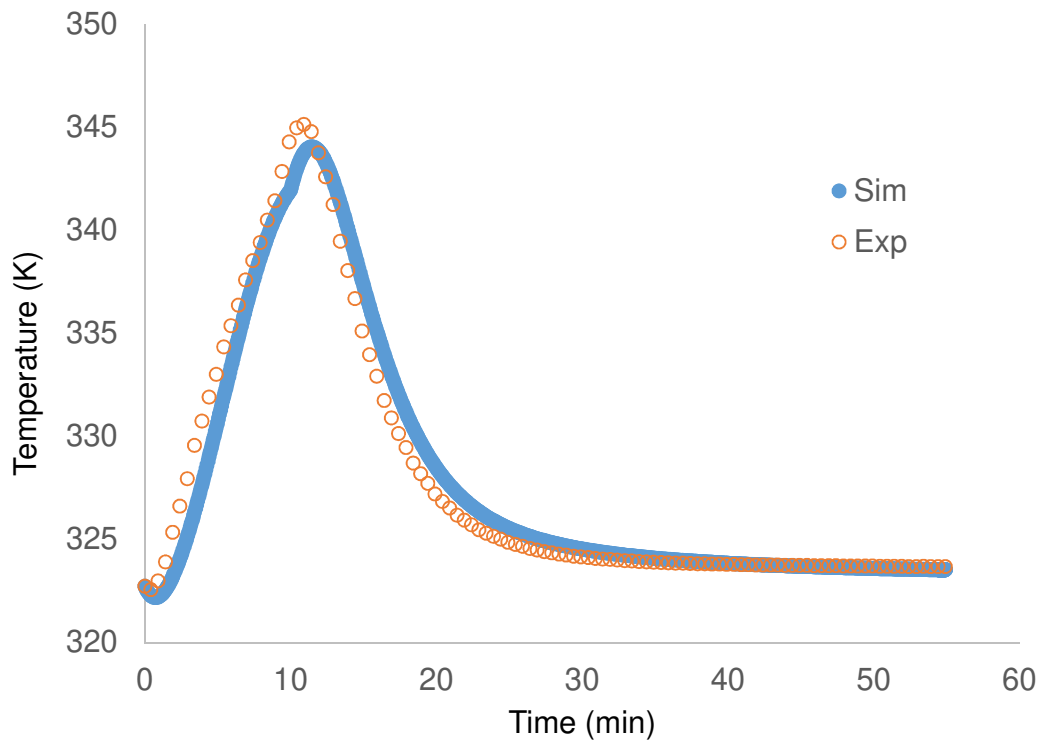
317 The coefficient of determination was expressed as

318
$$R^2 = 1 - \frac{(y_i - \hat{y}_i)^2}{(y_i - \bar{y})^2} \quad (33)$$

319

320

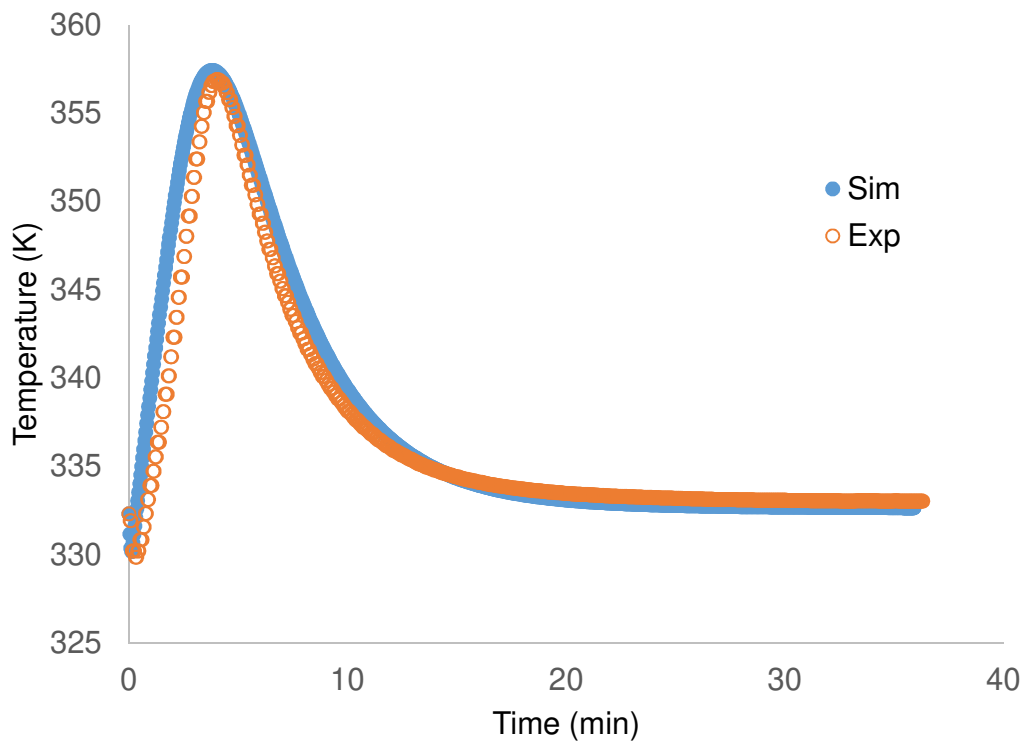
321 Figs. 7-8 show the fitting of the model to the experimental data for Runs 5 and 4. One can
322 notice that the model fits the experimental data. The value of the coefficient of determination
323 was found to be 99.15%. The reliability of the developed model is confirmed by the parity plot
324 (Fig. 9).



325

326

Fig. 7. Fitting of the model to the experimental data for Run 5.

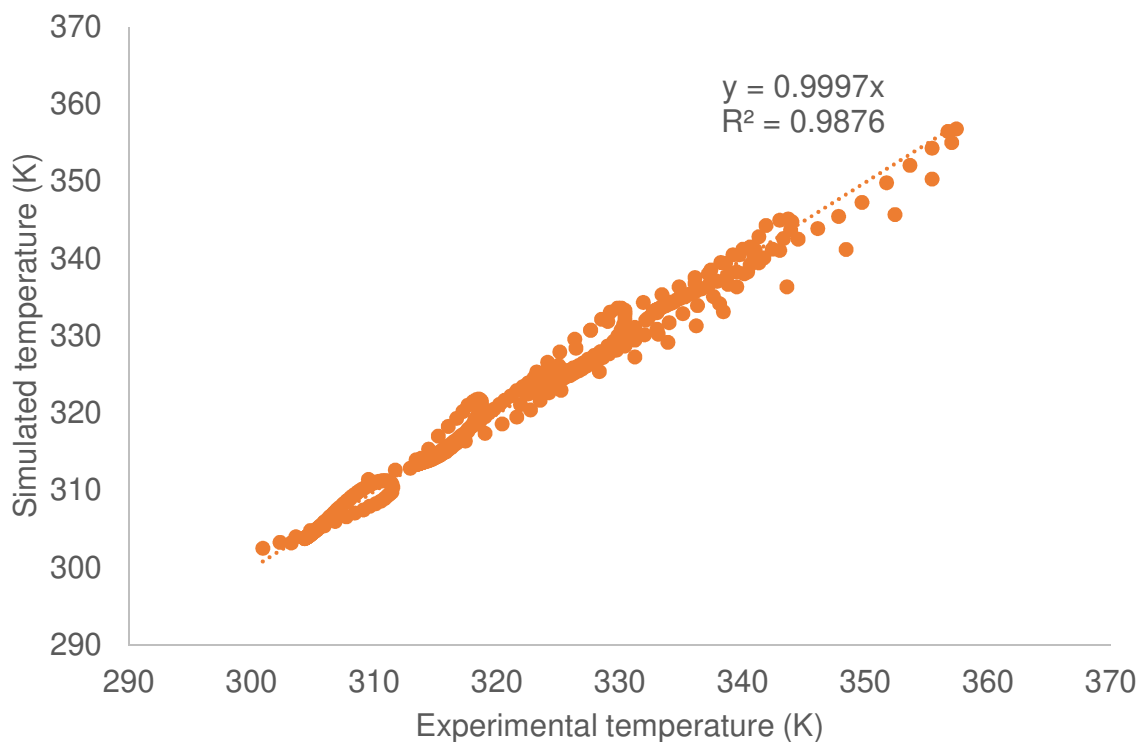


327

328

Fig. 8. Fitting of the model to the experimental data for Run 4.

329



330

331

Fig. 9. Parity plot.

332

333 Table 4 shows the values of the estimated kinetic constants for both routes. One can notice that
 334 the standard deviation values are very low for the non-catalyzed route but higher for the
 335 catalyzed ones. This difference can be explained by the fact that the reaction mechanism might
 336 be more complex than the one derived. Nevertheless, these standard error values are acceptable.

337 As expected, activation energy for the catalyzed route is lower than for the non-catalyzed one.

338 One should keep in mind that the rate constant for the catalyzed routes was lumped with an
 339 equilibrium constant.

340 A direct comparison with the other kinetic model, displayed in Table 5, cannot be done

341 because the expression of reaction rate was not the same. Zogg et al. [25] proposed a first order

342 reaction rate with respect to acetic anhydride and did not take into account the autocatalytic

343 effect, neither the catalytic effect of hydrochloric acid. The kinetic constants for the non-
 344 catalytic phenomenon estimated in this work can be compared with the ones obtained from
 345 References [20], [22] and [23] by keeping in mind that in these references the autocatalytic
 346 effect was not taken into account.

347 The activation energy, $Ea_{Hydrolysis-non.cat}$, was found to be in the same range than
 348 References [20] and [22] but lower than the one estimated in Reference [25]. The rate
 349 constants at 40°C was calculated to be: $k(40^\circ\text{C})= 2.23 \cdot 10^{-4} \text{ L mol}^{-1} \text{ s}^{-1}$ for [20], $k(40^\circ\text{C})=$
 350 $2.85 \cdot 10^{-5} \text{ L mol}^{-1} \text{ s}^{-1}$ for [23] and $k(40^\circ\text{C})= 6.60 \cdot 10^{-5} \text{ L mol}^{-1} \text{ s}^{-1}$ for [22]. Hence, the kinetic
 351 constants for the non-catalytic effect estimated in this work are closer to the ones estimated by
 352 Susanne et al. [22].

353 **Table 4**

354 **Estimated kinetic constants with $T_{ref}=313.15\text{K}$.**

Kinetic constants	Units	Estimated Parameters	Standard Error %
$k'_{Hydrolysis-cat}(T_{ref})$	$\text{L mol}^{-1} \text{ s}^{-1}$	$0.983 \cdot 10^{-1}$	17.9
$Ea_{Hydrolysis-cat}$	J mol^{-1}	29700	25.4
$k_{Hydrolysis-non.cat}(T_{ref})$	$\text{L mol}^{-1} \text{ s}^{-1}$	$0.250 \cdot 10^{-04}$	4.6
$Ea_{Hydrolysis-non.cat}$	J mol^{-1}	46000	4.3

355

356

357

358

359

360 **Table 5**

361 Kinetic constants reported in the literature.

Reference	Added catalyst	Reaction rate	k(s ⁻¹) at 40°C	Ea (kJ mol ⁻¹)
Zogg et al. [25]	HCl	$k(T) \times [\text{Acetic anhydride}]$	8.20·10 ⁻⁰³	56
			A (L mol⁻¹ s⁻¹)	Ea(kJmol⁻¹)
Asprey et al. [20]	None	$A \times e^{\frac{-Ea}{R.T}} \times ([\text{Acetic anhydride}] \times [\text{H}_2\text{O}])$	2121.75	41.84
Hirota et al. [23]	None	$A \times e^{\frac{-Ea}{R.T}} \times ([\text{Acetic anhydride}] \times [\text{H}_2\text{O}])$	19842433.99	71
Susanne et al. [22]	None	$A \times e^{\frac{-Ea}{R.T}} \times ([\text{Acetic anhydride}] \times [\text{H}_2\text{O}])$	3133.79	46.02

362

363 Another interesting comparison is between the kinetics of water and acetic anhydride,
364 methanol and acetic anhydride. Wei et al. [37] developed a kinetic model for the esterification
365 of acetic anhydride and methanol by taking into account the side reactions of acetic acid
366 esterification by methanol and acetic anhydride hydrolysis. They found that the activation
367 energy for the reaction between acetic anhydride and methanol is 88.07 kJ mol⁻¹, which is
368 higher than the one between water and acetic anhydride. Hence, the nucleophilic attack by
369 water is faster than by methanol.

370

371

372

373

374 3.7. Validation of the model with RC1

375 Similar experiments were performed in RC1 in order to compare the estimated constant in an
376 established calorimeter. The use of RC1 calorimeter system allows to have the evolution of
377 q_{loss} , C_{PR} and UA with time.

378 The coefficient of determination was found to be 93.44%, which is slightly lower than the
379 previous one.

380 Table 6 shows that the estimated kinetics are similar than the one obtained in handmade
381 reactor, showing the reliability of this latter system.

382 **Table 6**
383 Estimated kinetic constants with RC1 and $T_{\text{ref}}=313.15\text{K}$.
384

Kinetic constants	Units	Estimated parameter	Standard error %
$k'_{\text{Hydrolysis-cat}}(T_{\text{ref}})$	$\text{L mol}^{-1} \text{s}^{-1}$	0.105	29.2
$Ea_{\text{Hydrolysis-cat}}$	J mol^{-1}	29600	45.3
$k_{\text{Hydrolysis-non.cat}}(T_{\text{ref}})$	$\text{L mol}^{-1} \text{s}^{-1}$	$0.279 \cdot 10^{-04}$	5.0
$Ea_{\text{Hydrolysis-non.cat}}$	J mol^{-1}	42100	11.0

385

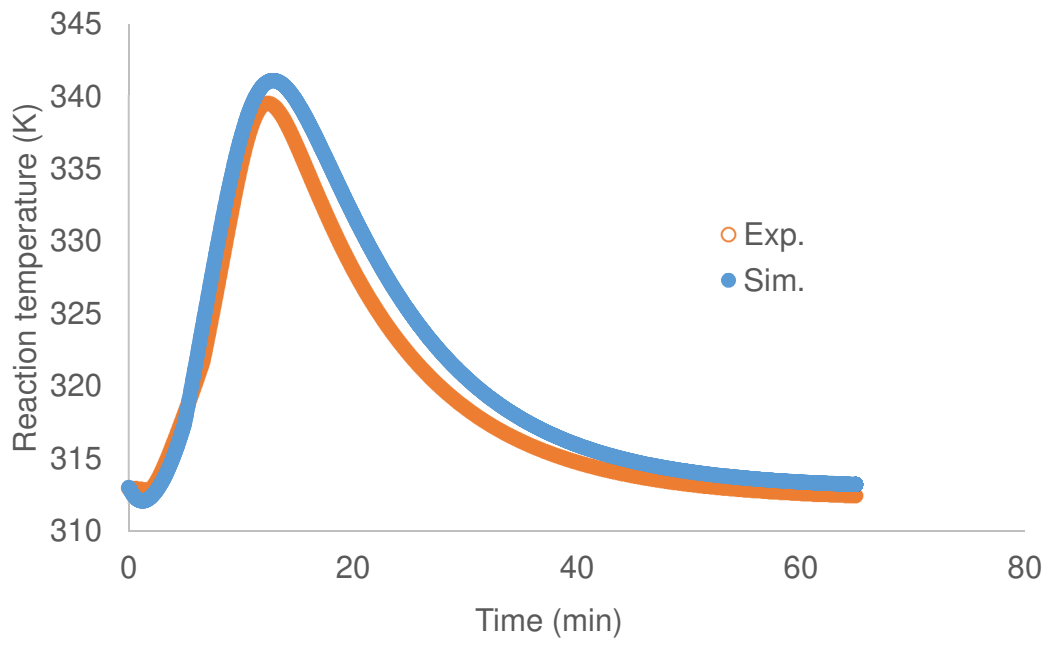
386 Fig. 10 shows the fitting of experimental temperature by the simulation for Run 7.

387

388

389

390



391

392

Fig. 10. Fitting of the model to the experimental data for Run 7.

393

394

395

396

397 **4. CONCLUSIONS**

398 This study proposes a revisited kinetic study of the hydrolysis of acetic anhydride by using
399 temperature as an online signal.

400 A hand-made calorimeter was thermally characterized to be able to evaluate the heat transfer
401 coefficient, specific heat capacity of the inserts and heat loss. Kinetic experiments were
402 performed under isoperibolic and semibatch mode. To develop a kinetic model, the following
403 parameters were varied: time of addition, initial reaction temperature and amount of acetic
404 anhydride added into the reactor.

405 The kinetic model, using the handmade calorimeter, was developed by taking into account two
406 routes: non-catalyzed and the catalyzed reaction due to the dissociation of the product acetic
407 acid. The following thermal phenomena were also included: reaction enthalpy, mixing
408 enthalpies and heat loss. It was found that the activation energy of the catalyzed route is lower
409 than the non-catalyzed one.

410 To validate the results found in handmade calorimeter, experiments were performed in RC1.
411 The estimated kinetic constants in RC1 were similar to the one in the handmade calorimeter.

412

413

414

415

416

417 **NOMENCLATURE**

\bar{C}_P	Capacity per mol, J mol ⁻¹ K ⁻¹
[<i>i</i>]	Concentration of compound <i>i</i>
\hat{C}_P	Capacity per mass, J g ⁻¹ K ⁻¹
<i>d</i>	Diameter, m
<i>E_a</i>	Activation energy, J mol ⁻¹
<i>k</i>	Rate constant, L mol ⁻¹ s ⁻¹
<i>K</i>	Equilibrium constant
<i>K^C</i>	Dissociation constant
<i>K^T</i>	Thermodynamic constant
<i>m</i>	Mass, kg
<i>N</i>	Rotating speed, rps
<i>Q</i>	Volumetric flow rate, L s ⁻¹
<i>q_{acc}</i>	Accumulated heat-flow rate, J s ⁻¹
<i>q_{dosing}</i>	Heat-flow rate due to dosing, J s ⁻¹
<i>q_{exchange with heat carrier}</i>	Heat-flow rate exchange with heat carrier, J s ⁻¹
<i>q_{loss}</i>	Heat-flow rate loss, J s ⁻¹

q_{reaction} Heat-flow rate due to chemical reaction, J s^{-1}

$q_{\text{solvation}}$ Heat-flow rate of solvation, J s^{-1}

R_i Reaction rate, $\text{mol L}^{-1} \text{s}^{-1}$

t Time, s

T Temperature, K

UA Overall heat-transfer coefficient, W K^{-1}

V Volume, L

ΔH Enthalpy, J mol^{-1}

$1/h$ Convective resistance, $\text{K m}^{-2} \text{W}^{-1}$

Greek letters

μ Dynamic viscosity, $\text{kg m}^{-1} \text{s}^{-1}$

λ Thermal conductivity, $\text{W m}^{-1} \text{K}^{-1}$

ω Mass fraction

ρ Density, kg m^{-3}

Subscripts

0	Time zero
ambient	Ambient
Cat.	catalyzed reaction
feed	Feed
Hydrolysis-cat.	catalyzed hydrolysis reaction
Hydrolysis-non.cat	non-catalyzed hydrolysis reaction
<i>i</i>	Component <i>i</i>
ins	inserts
<i>j</i>	Jacket
R	Reaction system
s	Stirrer
w	Wall
<i>Ref.</i>	Reference

418 **ACKNOWLEDGEMENTS**

419 This study has been done in the framework of Task 2: “Green process: 2nd generation of
420 biomass” of AMED project. The authors thank AMED project. The AMED project has been
421 funded with the support from the European Union with the European Regional Development
422 Fund (ERDF) and from the Regional Council of Normandie. The authors express their
423 gratitude to Prof. Johan Wärnå for his help in the modeling stage. The authors thank the
424 Ministry of High Education, Science and Technology of Dominican Republic. The authors
425 thank the “Programme Excellence Eiffel”.

426 **REFERENCES**

427 [1] X. Cai, K. Ait Aissa, L. Estel, S. Leveneur, Investigation of the Physicochemical
428 Properties for Vegetable Oils and Their Epoxidized and Carbonated Derivatives, *J. Chem. Eng.*
429 *Data*. 63 (2018) 1524–1533. doi:10.1021/acs.jced.7b01075.

430 [2] Q. Xu, J. Ding, S. Yang, S. Ye, Measurement and calculation method of changing heat
431 capacities during the reaction, *Thermochim. Acta*. 675 (2019) 55–62.
432 doi:10.1016/j.tca.2019.03.004.

433 [3] E. Hanitzsch, Messung der spezifischen wärmekapazität - vergleich zwischen DSC-
434 und pulsmethode, *Thermochim. Acta*. 151 (1989) 289–293. doi:10.1016/0040-6031(89)85357-
435 2.

436 [4] S.Q. Miao, H.P. Li, G. Chen, Temperature dependence of thermal diffusivity, specific
437 heat capacity, and thermal conductivity for several types of rocks, *J. Therm. Anal. Calorim.*
438 115 (2014) 1057–1063. doi:10.1007/s10973-013-3427-2.

439 [5] W.Y. Pérez-Sena, X. Cai, N. Kebir, L. Vernières-Hassimi, C. Serra, T. Salmi, S.
440 Leveneur, Aminolysis of cyclic-carbonate vegetable oils as a non-isocyanate route for the
441 synthesis of polyurethane: A kinetic and thermal study, *Chem. Eng. J.* 346 (2018) 271–280.
442 doi:10.1016/j.cej.2018.04.028.

443 [6] I. Bylina, L. Trevani, S.C. Mojumdar, P. Tremaine, V.G. Papangelakis, Measurement of
444 reaction enthalpy during pressure oxidation of sulphide minerals, *J. Therm. Anal. Calorim.* 96
445 (2009) 117–124. doi:10.1007/s10973-008-9883-4.

- 446 [7] R. André, M. Giordano, C. Mathonat, R. Naumann, A new reaction calorimeter and
447 calorimetric tools for safety testing at laboratory scale, *Thermochim. Acta.* 405 (2003) 43–50.
448 doi:10.1016/S0040-6031(03)00129-1.
- 449 [8] S. Leveneur, M. Pinchard, A. Rimbault, M. Safdari Shadloo, T. Meyer, Parameters
450 affecting thermal risk through a kinetic model under adiabatic condition: Application to liquid-
451 liquid reaction system, *Thermochim. Acta.* 666 (2018) 10–17. doi:10.1016/j.tca.2018.05.024.
- 452 [9] K.-Y. Chen, S.-H. Wu, Y.-W. Wang, C.-M. Shu, Runaway reaction and thermal
453 hazards simulation of cumene hydroperoxide by DSC, *J. Loss Prev. Process Ind.* 21 (2008)
454 101–109. doi:10.1016/j.jlp.2007.09.002.
- 455 [10] A. Keller, D. Stark, H. Fierz, E. Heinzle, K. Hungerbühler, Estimation of the time to
456 maximum rate using dynamic DSC experiments, *J. Loss Prev. Process Ind.* 10 (1997) 31–41.
457 doi:10.1016/S0950-4230(96)00037-X.
- 458 [11] O.R. Valdes, V.C. Moreno, S. Waldram, L. Véchet, M.S. Mannan, Runaway
459 decomposition of dicumyl peroxide by open cell adiabatic testing at different initial conditions,
460 *Process Saf. Environ. Prot.* 102 (2016) 251–262. doi:10.1016/j.psep.2016.03.021.
- 461 [12] Y. Wang, L. Vernières-Hassimi, V. Casson-Moreno, J.-P. Hébert, S. Leveneur, Thermal
462 Risk Assessment of Levulinic Acid Hydrogenation to γ -Valerolactone, *Org. Process Res. Dev.*
463 22 (2018) 1092–1100. doi:10.1021/acs.oprd.8b00122.
- 464 [13] A. Zogg, F. Stoessel, U. Fischer, K. Hungerbühler, Isothermal reaction calorimetry as a
465 tool for kinetic analysis, *Thermochim. Acta.* 419 (2004) 1–17. doi:10.1016/j.tca.2004.01.015.

- 466 [14] L. Vernières-Hassimi, A. Dakkoune, L. Abdelouahed, L. Estel, S. Leveneur, Zero-
467 Order Versus Intrinsic Kinetics for the Determination of the Time to Maximum Rate under
468 Adiabatic Conditions (TMRad): Application to the Decomposition of Hydrogen Peroxide, *Ind.*
469 *Eng. Chem. Res.* 56 (2017) 13040–13049. doi:10.1021/acs.iecr.7b01291.
- 470 [15] E. Marco, S. Cuartielles, J.A. Peña, J. Santamaria, Simulation of the decomposition of
471 di-cumyl peroxide in an ARSST unit, *Thermochim. Acta.* 362 (2000) 49–58.
472 doi:10.1016/S0040-6031(00)00587-6.
- 473 [16] I. Dobrosavljevic, E. Schaer, J.M. Commenge, L. Falk, Intensification of a highly
474 exothermic chlorination reaction using a combined experimental and simulation approach for
475 fast operating conditions prediction, *Chem. Eng. Process. Process Intensif.* 105 (2016) 46–63.
476 doi:10.1016/j.cep.2016.04.007.
- 477 [17] M.J. Todd, J. Gomez, Enzyme kinetics determined using calorimetry: a general assay
478 for enzyme activity?, *Anal. Biochem.* 296 (2001) 179–187. doi:10.1006/abio.2001.5218.
- 479 [18] W. Hoffmann, Y. Kang, J.C. Mitchell, M.J. Snowden, Kinetic Data by Nonisothermal
480 Reaction Calorimetry: A Model-Assisted Calorimetric Evaluation, *Org. Process Res. Dev.* 11
481 (2007) 25–29. doi:10.1021/op060144j.
- 482 [19] T.J. Snee, C. Bassani, J.A.M. Lighthart, Determination of the thermokinetic parameters
483 of an exothermic reaction using isothermal, adiabatic and temperature-programmed
484 calorimetry in conjunction with spectrophotometry, *J. Loss Prev. Process Ind.* 6 (1993) 87–94.
485 doi:10.1016/0950-4230(93)90005-I.

- 486 [20] S.P. Asprey, B.W. Wojciechowski, N.M. Rice, A. Dorcas, Applications of temperature
487 scanning in kinetic investigations: The hydrolysis of acetic anhydride, *Chem. Eng. Sci.* 51
488 (1996) 4681–4692. doi:10.1016/0009-2509(96)00306-5.
- 489 [21] F.L. Wiseman, New insight on an old reaction – the aqueous hydrolysis of acetic
490 anhydride, *J. Phys. Org. Chem.* 25 (2012) 1105–1111. doi:10.1002/poc.2945.
- 491 [22] F. Susanne, D.S. Smith, A. Codina, Kinetic Understanding Using NMR Reaction
492 Profiling, *Org. Process Res. Dev.* 16 (2012) 61–64. doi:10.1021/op200202k.
- 493 [23] W.H. Hirota, R.B. Rodrigues, C. Sayer, R. Giudici, Hydrolysis of acetic anhydride:
494 Non-adiabatic calorimetric determination of kinetics and heat exchange, *Chem. Eng. Sci.* 65
495 (2010) 3849–3858. doi:10.1016/j.ces.2010.03.028.
- 496 [24] A. Zogg, U. Fischer, K. Hungerbühler, A New Small-Scale Reaction Calorimeter That
497 Combines the Principles of Power Compensation and Heat Balance, *Ind. Eng. Chem. Res.* 42
498 (2003) 767–776. doi:10.1021/ie0201258.
- 499 [25] A. Zogg, U. Fischer, K. Hungerbühler, A new approach for a combined evaluation of
500 calorimetric and online infrared data to identify kinetic and thermodynamic parameters of a
501 chemical reaction, *Chemom. Intell. Lab. Syst.* 71 (2004) 165–176.
502 doi:10.1016/j.chemolab.2004.01.025.
- 503 [26] M.Á. Gómez García, I. Dobrosz-Gómez, J.C. Ojeda Toro, Thermal stability and
504 dynamic analysis of the acetic anhydride hydrolysis reaction, *Chem. Eng. Sci.* 142 (2016) 269–
505 276. doi:10.1016/j.ces.2015.12.003.

- 506 [27] N. Asiedu, D. Hildebrandt, D. Glasser, Kinetic Modeling of the Hydrolysis of Acetic
507 Anhydride at Higher Temperatures using Adiabatic Batch Reactor (Thermos-Flask), in: 2013.
508 doi:10.4172/2157-7048.1000176.
- 509 [28] J.L. Zheng, J. Wärnå, T. Salmi, F. Burel, B. Taouk, S. Leveneur, Kinetic modeling
510 strategy for an exothermic multiphase reactor system: Application to vegetable oils epoxidation
511 using Prileschajew method, *AIChE J.* 62 (2016) 726–741. doi:10.1002/aic.15037.
- 512 [29] S. Leveneur, M. Thönes, J.-P. Hébert, B. Taouk, T. Salmi, From Kinetic Study to
513 Thermal Safety Assessment: Application to Peroxyformic Acid Synthesis, *Ind. Eng. Chem.*
514 *Res.* 51 (2012) 13999–14007. doi:10.1021/ie3017847.
- 515 [30] I. Dobrosavljevic, E. Schaer, J.M. Commenge, L. Falk, Intensification of a highly
516 exothermic chlorination reaction using a combined experimental and simulation approach for
517 fast operating conditions prediction, *Chem. Eng. Process. Process Intensif.* 105 (2016) 46–63.
518 doi:10.1016/j.cep.2016.04.007.
- 519 [31] K. Sue, F. Ouchi, K. Minami, K. Arai, Determination of Carboxylic Acid Dissociation
520 Constants to 350 °C at 23 MPa by Potentiometric pH Measurements, *J. Chem. Eng. Data.* 49
521 (2004) 1359–1363. doi:10.1021/je049923q.
- 522 [32] S. Leveneur, L. Vernieres-Hassimi, T. Salmi, Mass & energy balances coupling in
523 chemical reactors for a better understanding of thermal safety, *Educ. Chem. Eng.* 16 (2016)
524 17–28. doi:10.1016/j.ece.2016.06.002.

525 [33] <http://www.stenutz.eu/chem/solv6.php?name=acetic%20anhydride>, acetic anhydride,
526 (n.d.). <http://www.stenutz.eu/chem/solv6.php?name=acetic%20anhydride> (accessed June 29,
527 2019).

528 [34] F. Lavanchy, Development of reaction calorimetry applied to supercritical CO₂ and
529 methanol-CO₂ critical mixture, Infoscience. (2005). doi:10.5075/epfl-thesis-3228.

530 [35] H. Rakotondramaro, J. Wärnä, L. Estel, T. Salmi, S. Leveneur, Cooling and stirring
531 failure for semi-batch reactor: Application to exothermic reactions in multiphase reactor, J.
532 Loss Prev. Process Ind. 43 (2016) 147–157. doi:10.1016/j.jlp.2016.05.011.

533 [36] H. Haario, MODEST-User's Guide, (2001).

534 [37] H.-Y. Wei, Z.-C. Guo, L. Hao, W.-S. Bai, R. Wang, S. Li, identification of the kinetic
535 parameters and autocatalytic behavior in esterification via isoperibolic reaction calorimetry,
536 Org. Process Res. Dev. 20 (2016) 1416-1423. doi: 10.1021/acs.oprd.5b00395

537

538

539

540